

EFFECT OF CARBON CONTENT ON THE STRUCTURE AND MICROHARDNESS OF STEELS UNDER RAPID ACTION BY DEFORMING CUTTING

O. M. Zhigalina,^{1,2} A. G. Degtyareva,² N. N. Zubkov,² V. N. Simonov,² and S. G. Vasil'ev²

Translated from *Metallovedenie i Termicheskaya Obrabotka Metallov*, No. 2, pp. 65 – 71, February, 2020.

The effect of deforming cutting (DC) on structural and phase transformations in iron and steels 35 and U8 is studied with the help of scanning optical and transmission electron microscopy. It is shown that with an increase in carbon content test material structure and phase composition become more complex.

Key words: strain hardening, deforming cutting, effect of carbon, hardened structures.

INTRODUCTION

Surface hardening is a most effective and economic method of improving component wear resistance. Currently there are tens of surface hardening techniques the majority of which require specialized heat treatment equipment in order to accomplish structural and phase transformations. A relatively new method for surface strengthening is hardening directly in metal cutting equipment. The temperatures required for hardening are achieved during cutting due to plastic deformation and friction in the tool and workpiece contact area. Combined action of high degrees of deformation, high local temperatures and cooling rates, lead to a situation that the treated surface experiences structural changes [1]. Hardening in metal cutting lathes may be performed both with a cutter and also with an abrasive tool. The effect of hardened layer preparation during turning has been described in [2, 3]. With high-speed cutting by a tool made of ultrahard material apart from deformation strengthening structural and phase transformations are also observed within a workpiece surface layer [4].

The effect of hardening by grinding was described for the first time in 1994 [5]. Whereas hardening cutting was not within the scope of experimental studies, hardening grinding is used in industry. Currently specialized machining centers are produced in order to implement this process [6]. In order

to intensify heat release there is use of forced grinding regimes with a considerable cutting depth, from 0.2 to 1.2 mm. Rapid cooling is achieved due to passage of heat into the underlying layers. Use of cooling liquids is not obligatory [7]. The hardening depth after removal of a defective layer is from 0.3 – 0.5 mm with a surface hardness achieved of 50 – 60 HRC. The heat-affected zone reaches 2 mm [8, 9].

Almost all of the power required is the main drive of the turning and grinding lathe comprising units of kilowatts consumed in heating a cutting zone, which may have a volumes of units or tenths of a cubic millimeter. For example, during turning of steel AISI 1045 with a cutting rate of 2.7 m/sec the temperature in the cutting zone reach 1030°C with a degree of deformation up to 400% and deformation rate up to 10^4 sec^{-1} . The heating rate may be up to 10^6 K/sec with a cooling rate of 10^3 K/sec [10]. These conditions lead to a situation that during cutting structure and phase transformations proceed within the turning itself.

Use of the method of deformation cutting (DC) has been described in [11] in order to obtain a hardened structure in steel cylindrical surfaces according to a patent [12]. A diagram of the strengthening process is given in Fig. 1 [11].

The tool used is a cutter with special geometry for its cutting and deforming section. Cut layers do not separate entirely from a workpiece and remain upon it retaining a strong mechanical bond with a machined surface. In the outer surface of a workpiece there is a deformed layer in the form of inclined fins densely pressed to each other (Fig. 2).

With DC rates of 3 – 5 m/sec the mean integral temperature in the treatment area measured by a natural thermocouple reaches 1100°C. Thermocouple elements are the different

¹ A. V. Shubnikov Institute of Crystallography, Federal Scientific and Research Center “Crystallography and Photonics,” Russian Academy of Sciences, Moscow, Russia.

² N. É. Bauman Moscow State Technical University (MGTU), Moscow, Russia (e-mail: dega_70@mail.ru).

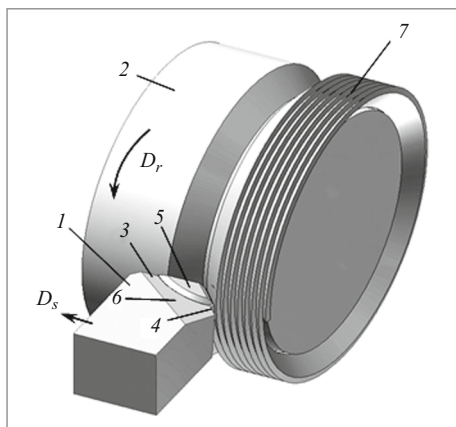


Fig. 1. Diagram of DC [11]: 1) tool for DC; 2) workpiece; 3) cutting edge; 4) deforming edge; 5) undercut layer; 6) tool leading surface; 7) strengthened edge.

materials of a component and cutting tool that during cutting have a heated contact being the junction of this thermocouple. Subsequent rapid cooling of an undercut layer with heat released into the core of a workpiece leads to preparation within a deformed fin of a hardened structure. The main sources of heat liberation are the intense plastic deformation in the DC zone and friction of an undercut layer sliding over an active area of the tool leading surface. With a cutting rate of 3 m/sec and length of the heat liberation section of 1.2 mm the heating time is 4.0×10^{-4} sec. It has also been shown in [13] that the material heating rate for the undercut layer comprises up to 2.7×10^6 K/sec. The volumetric density of power determined as the ratio of DC power to the volume of material consumption subjected to treatment comprises 8.0 kJ/cm^3 with overall heat liberation power of 2.4 kW. In this case the cooling rate is estimated as 10^4 K/sec.

The aim of the present work is to study phase and structural transformation proceeding within commercial grade iron and steels with a different carbon content with high-speed heat treatment during deforming cutting.

METHODS OF STUDY

Features of the effect of carbon content on structure and phase transformation during DC were studied in commercial grade iron containing less than 0.05% carbon, steel 35 containing 0.38% carbon, and steel U8 containing 0.85% carbon. In order to analyze the behavior of ferrite during DC commercial grade iron was used, and the behavior of pearlite was revealed for steel U8.

Test specimens were subjected to high-speed quenching during the DC process in the faculty of instrumental engineering and technology of the N. É. Bauman MGTU. The DC rate $v = 3.3 - 3.5$ m/sec, cutting depth $t = 0.6 - 1$ mm, and feed $S = 0.05 - 0.1$ mm/rev.

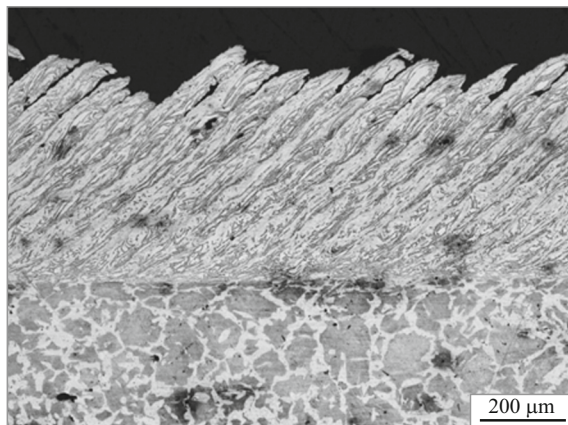


Fig. 2. Typical strengthened surface structure with densely packed fins obtained by DC (steel 35).

A study of specimen structure and phase composition was performed comprehensively using light, scanning, and transmission electron microscopy. Metallographic analysis of the surface of microsections was accomplished in an Olympus GX51 microscope at magnification up to $\times 1000$. In order to reveal the structure of a microsection surface it was etched in 4% HNO_3 in $\text{C}_2\text{H}_5\text{OH}$. Specimen microhardness was measured in an EMCO TEST Durascan microhardness meter with a load of 0.5 N (50 g) and 1 N (100 g) SEM images of the surface of specimens was obtained by means of a VEGA TESCAN 10 20 kV electron microscope in a secondary electron regime. Transmission electron microscopy (TEM), transmission scanning microscopy (TSEM) were carried out by means of a Tecnai Osiris microscope with an accelerating voltage of 200 kV.

Specimens for TEM were prepared in the form of foil by mechanical polishing and electrochemical etching, and they were also cut with an ion beam in the column of an FEI Scios microscope.

RESULTS

Commercial grade iron. The microstructure of commercial grade iron is shown in Fig. 3 before (Fig. 3a) and after (Fig. 3b) DC. Quantitative metallographic data are provided in Table 1. Calculation of the size of ferrite grains showed that DC treatment leads to refinement of ferrite grains by a factor of 20. This structure has increased microhardness that comprises $250 - 260 \text{ HV}_{0.1}$ (before DC 150 it is $150 \text{ HV}_{0.1}$). Probably during DC there is dynamic recrystallization leading to preparation of a dispersed ferrite structure.

At the base of a surface layer with a finned microstructure from the direction of the fin surface, which during DC is subjected to less deformation, light areas may be observed (Fig. 4, shown by arrows) with increased microhardness, i.e., up to $310 \text{ HV}_{0.05}$. This is probably sections where there was no recrystallization.

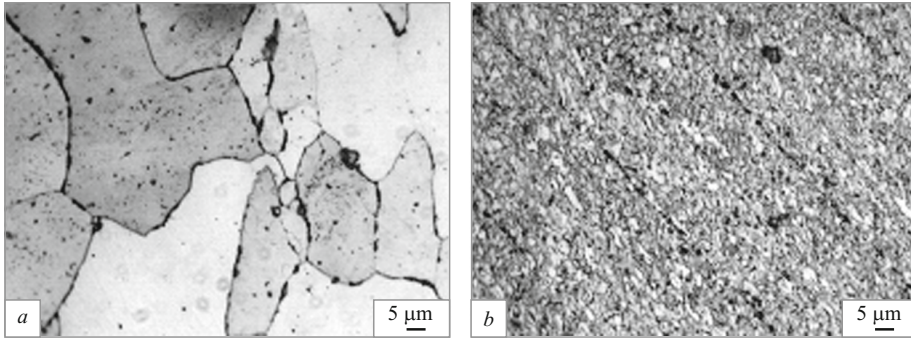


Fig. 3. Ferrite grain in commercial grade iron before (a) and after (b) DC treatment.

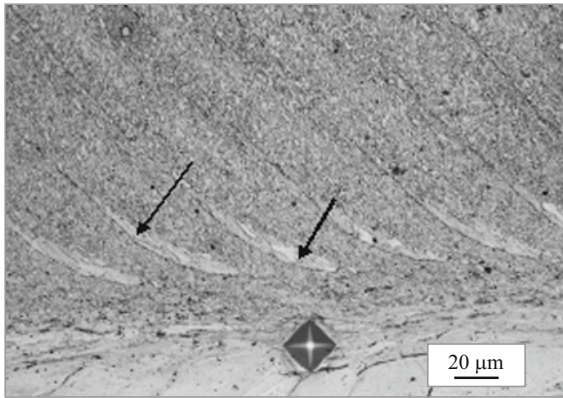


Fig. 4. Microstructure of commercial grade iron at the base of a finned surface after DC ($v = 3.6$ m/sec; $S_0 = 0.05$ mm/rev; $t = 1$ mm; light deformed areas marked with arrows).

Therefore, these metallographic studies have shown that commercial grade iron as a result of DC treatment may have an equiaxed recrystallized structure with a different degree of fineness and a deformed fibrous structure or a combination of them.

Steel 35. In medium-carbon steels it is possible to obtain a larger spectrum of structures due to the fact that according to the Fe – C composition diagram with an increase in steel carbon content there is a reduction in Ac_3 critical point. Apart from deformed structures as a result of DC treatment quenched structures are observed. It is seen in Fig. 5a that the cutting zone (this is part of the undercut layer experiencing intense friction in contact with a tool, noted by arrow 1) has a structure differing from that of a free zone (this is part of the undercut layer not in contact with a tool noted by arrow 2). This difference is connected with the fact that the undercut zone is heated above the Ac_1 critical temperature and

correspondingly experiences phase transformation of pearlite into austenite ($P \rightarrow A$). As a result of this transformation leads to preparation in an undercut zone of fine structures of incomplete hardening. The remaining part of a fin retains a deformed fibrous structure. Microhardness in the cut zone of a fin comprises $520 HV_{0.1}$ and in the free zone it is $360 HV_{0.1}$. The microhardness of a cut area may reach about $600 HV_{0.1}$ as a result of the fact during treatment apart from $P \rightarrow A$ transformation there is polymorphic transformation of ferrite into austenite ($F \rightarrow A$). We have called these structures “partially hardened”.

Inheritance of a deformed structure, when fibers are directed predominantly along a fin of a treated layer, may be retained also during “through hardening” (Fig. 5b). This signifies that all of a fin (right through) during DC experiences hardening. In a cut area a structure is observed of complete hardening (without signs of residual ferrite), and in the free area there is incomplete hardening as a result of which ferrite is present of quite equiaxed shape (shown with arrows in Fig. 5b).

An SEM image is provided in Fig. 5c for the structure of cut and free areas of a fin where areas etched differently are seen. In the cut area martensite-like (ML) crystals are observed and in the free zone apart from ML-crystals ferrite (F) grains are present. The size of equiaxed ferrite grains is mainly $1.0 - 1.5 \mu\text{m}$, and martensite-like crystals of matrix phase are $1 - 3 \mu\text{m}$.

The average microhardness within the core not subjected to treatment is $250 HV_{0.1}$, and at the surface (treated layer) it reaches $650 - 670 HV_{0.1}$. In this case sections of fin free zone, including residual ferrite, have reduced microhardness of $550 HV_{0.1}$ and in ML-sections of a cut zone it is $710 HV_{0.1}$.

Under DC conditions the heating time is thousandths of a second, and therefore the phase transformation of pearlite at the Ac_1 temperature cannot be completed since carbon dissolution under these conditions is limited by atom diffusion mobility [14]. Studies of the surface layer structure by the SEM method (Fig. 6) after DC treatment of steel 45 showed that within fins there is insoluble cementite that is thinned, broken, and partly coagulates into areas of crystal splitting.

Therefore, the strengthened surface of medium-carbon steel treated by DC apart from a deformation structure may

TABLE 1. Results of Commercial Grade Iron Quantitative Metallography

Characteristics	Before DC	After DC
Number of ferrite grains	21	1009
Average ferrite grain size, μm	~ 20	~ 1

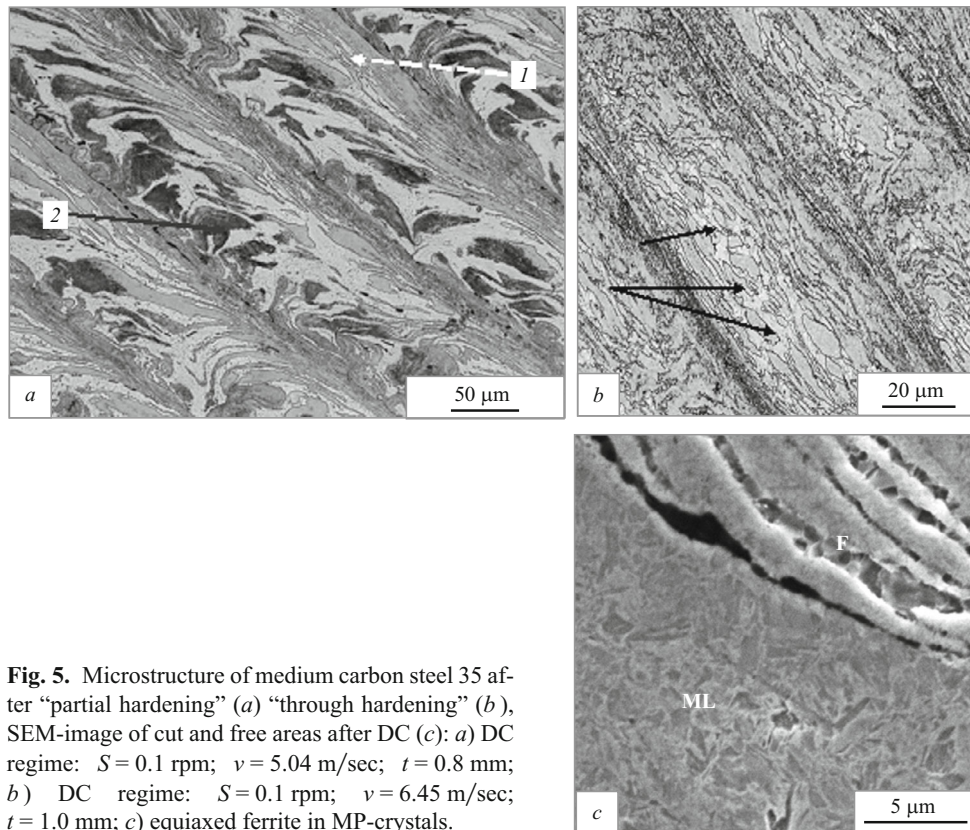


Fig. 5. Microstructure of medium carbon steel 35 after “partial hardening” (a) “through hardening” (b), SEM-image of cut and free areas after DC (c): a) DC regime: $S = 0.1$ rpm; $v = 5.04$ m/sec; $t = 0.8$ mm; b) DC regime: $S = 0.1$ rpm; $v = 6.45$ m/sec; $t = 1.0$ mm; c) equiaxed ferrite in MP-crystals.

have a combined structure of “partial hardening” and deformation or a structure of “through hardening”.

Steel U8. The original structure of a steel U8 workpiece with spheroidized pearlite provides preparation of microhardness at the level of $240 HV_{0.1}$. As research has shown, in this steel it is possible to observe a richer spectrum of structures after DC treatment. Similar to commercial grade iron and steel 35 a deformed structure is retained. The microhardness in the cutting zone of steel U8 may reach $570 HV_{0.1}$, whereas its average value in the deformed part of a fin is $380 HV_{0.1}$ (DC regime: $S = 0.2$ mm/rev, $v = 3.67$ m/sec, $t = 0.75$ mm).

It should be noted that with a change in cutter geometry the deformation structure is less expressed although the microhardness is unchanged. In the surface zone a light band

appears within which the microhardness increases sharply to $790 HV_{0.1}$. Apparently this is due to successive phase transformations “pearlite spheroidization – austenite – martensite”, implemented during hardening in the DC process. The width of a band depends to a considerable extent on cutting rate.

The uniform structure of steel U8 after DC is shown in Fig. 7a without signs of deformation and any changes in the cut zone. The average microhardness is about $900 HV_{0.1}$. This structure is apparently a result of “through hardening.”

It is interesting to note that in steel U8 DC treatment may also lead to preparation of an extremely nonuniform structure over the width of a fin (Fig. 7b): from the cutting zone side a layer is observed poorly subject to etching and consisting mainly of light smooth regions. The free zone of a fin

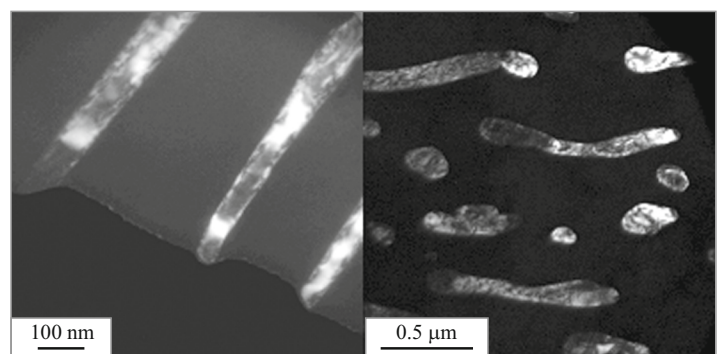


Fig. 6. Dark field SEM-images of cementite platelets of equal shape in steel 35 after DC.

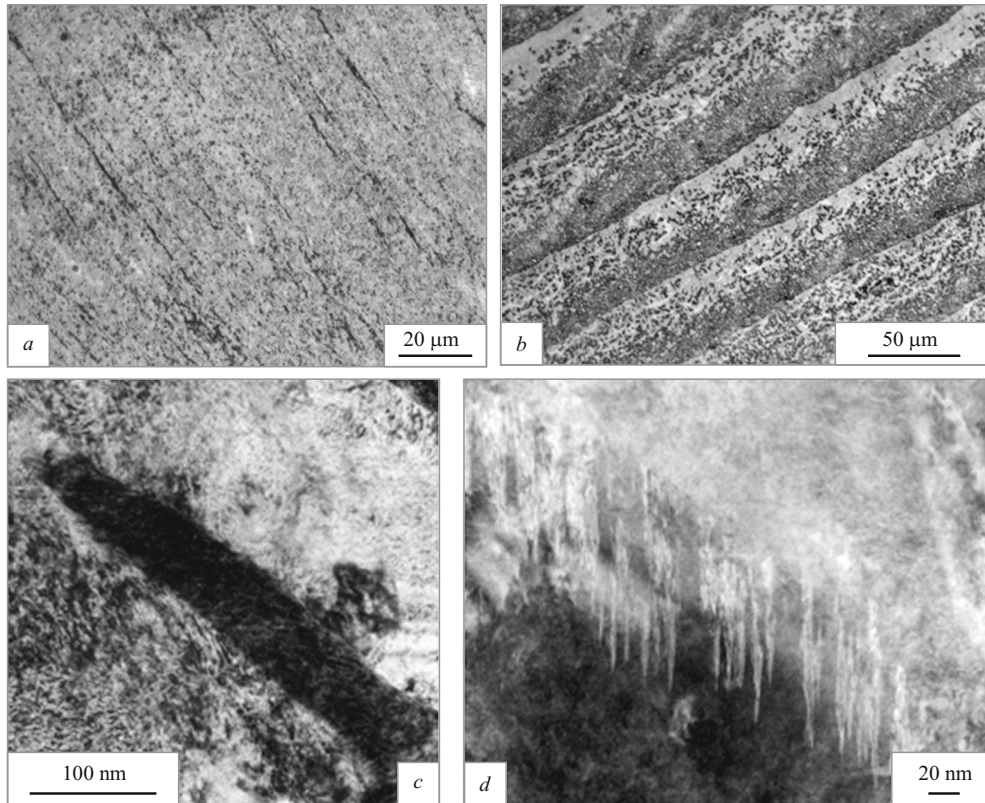


Fig. 7. Edge microstructure after “through hardening” (*a*), inhomogeneous structure (*b*), and cementite platelets (*c*, *d*) in steel U8 after DC: *a*) DC regime: $S = 0.05$ rpm; $v = 3.67$ m/sec; $t = 1$ mm; *b*) DC regime: $S = 0.05$ rpm; $v = 3.26$ m/sec; $t = 1$ mm; *c*) SEM-image of entirely insoluble cementite platelets; *d*) TSEM-image of fine nano-cementite platelets growing at a grain boundary.

conversely etches well and light areas within it are almost absent. However, in spite of the fundamental difference between the structure of the cutting and free zones their microhardness hardly differs ($630 HV_{0.1}$ in the cut zone and $550 HV_{0.1}$ in the free zone), whereas the microhardness of light regions is $900 HV_{0.1}$, which is higher by a factor of 1.5 than the average value for a fin (about $600 HV_{0.1}$).

As SEM studies have shown, this increase in hardness is connected with presence of cementite, not entirely dissolved (Fig. 7*c*) or newly formed (Fig. 7*d*) with formation of complex temperature gradients and deformation fields arising during DC.

DISCUSSION

During comparison of the microstructure of commercial grade iron, steels 45 and U8 before and after DC similarity has been revealed as well as a significant difference in the structural state of materials with a different carbon content.

The DC process is accompanied by considerable energy consumption in implementing cutting and friction, and a very high degree of plastic deformation during heating of the material surface treatment zone to high temperature (of the or-

der to 1100°C). Primarily there is very marked structure grain refinement. For example, a twenty-fold reduction in grain size of commercial grade iron is due to the ultra-high degree of deformation and short growth time, i.e., 4×10^{-4} sec.

Periodic structural inhomogeneity may clearly develop: the free zone of a fin differs with respect to structure and phase composition from the surface zone. This occurs due to the fact the temperature of the free zone forms due to a single factor, i.e., heat release during fin cutting. In the surface region a second factor is added, i.e., the force of friction during fin folding as a result of whose action dense packing is realized. These factors provided a higher temperature of the cut zone compared with the free zone. Judging from the difference in structures observed it exceeds the steel critical point that in combination with high-speed heat removal into a workpiece provides preparation of a hardened structure.

During a study of steel 35 attention is drawn to the particular dynamic flow of ductile ferrite grains. During deformation ferrite grains are drawn out over the length and thinned in a transverse direction. With distance from the boundary of the surface zone the efficiency of ferrite deformation decreases due to retarding processes of pearlite colonies, and there is a change in the direction of their deforma-

tion. Even with “through hardening” all of a fin retains ferrite grains that points to the inadequate time for diffusion redistribution of carbon within austenite during DC.

The nonuniform structure obtained for steel U8 is connected with the fact that with fast heating rates (about 10^6 K/sec) the temperature of critical points Ac_1 and Ac_3 , whose achievement is required in order to implement incomplete/complete hardening, increases by not less than 200°C . This signifies that in order to achieve although incomplete hardening the heating temperature should not be below 927°C . During hardening steel U8 in the DC process the free zone of a fin is not always heated to this temperature. In order to form and grow cementite crystals at the boundaries of grain during subsequent heating and cooling diffusion movement of carbon atoms from cementite dissolved in austenite is required. Evaluation of the diffusion path of carbon atoms showed that during a heating and cooling cycle, equal to 4×10^{-4} sec the distance that carbon atoms may overcome is about 60 nm. These nanocrystalline precipitates are shown in Fig. 7b.

CONCLUSIONS

Metallographic and electron microscope methods have been used to study the structure and phase composition of commercial grade iron and steels 35 and U8 subjected to deformation cutting. It has been established that in commercial grade iron DC leads to formation of an equiaxed recrystallized structure with a different degree of fineness, a deformed fibrous structure, or a combination of them. In this case the average grain size decreases from 20 to 1 μm , and the microhardness increases by a factor of 1.7 – 2.1.

In medium-carbon steel 35 apart from a deformed structure shows a structure of “partial” (with formation of martensite like crystals, untransformed ferrite and a deformed ferrite-pearlite mixture) and “through” hardening (martensite-like crystals, insoluble cementite and residual ferrite). Therefore, the steel 35 ferrite-pearlite structure after DC treatment is considerably complicated. In this case the maximum microhardness exceeds by a factor of 2.8 that in the original condition (after normalizing). The level of microhardness achieved corresponds to that obtained after standard hardening.

A feature of steel U8 is occurrence of more clearly expressed periodic structural inhomogeneity within a treated layer, probably connected with movement of critical points Ac_1 and Ac_3 in the direction of lower temperature as a result of material heating at an extremely fast rate. Crystals of nano-cementite are observed, growing from a grain boundary with width up to 10 nm. DC treatment leads to preparation of a microhardness exceeding the original more than a factor of 3.5.

Structural studies were partly conducted on equipment of the Federal Scientific and Research Center “Crystallography and Photonics,” Russian Academy of Sciences, with financial support of the Ministry and Science and Higher education within the scope of performing work according to a state assignment FNITs “Crystallography and photonics” Russian Academy of Sciences in the section for performing research by electron microscopy methods.

REFERENCES

1. Y. Guo and G. Janowski, “Microstructural characterization of white layers by hard turning and grinding,” *Trans. NAMRI/SME*, **XXXII**, 367 – 374 (2004).
2. Y. B. Guoanda and W. Warren, “Microscale mechanical behavior of the subsurface by finishing processes,” *ASME J. Manuf. Sci. Eng.*, No. 127, 333 – 338 (2004)
3. S. Naik, C. Guo, S. Malkin, et al., “Experimental investigation of hard turning,” in: *2nd Int. Mach. & Grinding Conf. Dearborn, MI* (1997), pp. 224 – 308.
4. J. Kundrak, A. Mamalis, K. Gyani, and V. Bana, “Surface layer microhardness changes with high-speed turning of hardened steels,” *Int. J. Adv. Manuf. Technol.*, **53**(1), 105 – 112 (2011).
5. E. Brinksmeier and T. Brockhoff, “Randschicht Wärmebehandlung durch Schleifen,” *Härterei-Techn. Mitt.*, **49**(5), 327 – 330 (1994).
6. G. Hyatt, “Integration of heat treatment into the process Chai-nofa Mill Turn Center by enabling external cylindrical grind-hardening,” *Prod. Eng.-Res. Devel. (WGP Annals)*, **7**(6), 571 – 584 (2013). (DOI: 10.1007/s11740-013-0465-3).
7. T. Nguyen, M. Liu, L. Zhang, et al., “An investigation of the grinding–hardening induced by traverse cylindrical grinding,” *ASME. Manuf. Sci. Eng.*, **136**(5), 051008–1 – 05100–10 (2014) (DOI: 10.1115/1.4028058).
8. L. Zhanqiang, X. Ai, and Z. Wang, “Comparison study of surface hardening by grinding versus machining,” *Key Engineering Materials*, **304 – 305**, 156 – 160 (2006).
9. X. Huang, Y. Ren, W. Wu, and T. Li, “Research on grind-hardening layer and residual stresses based on variable grinding forces,” *Int. J. Adv. Manuf. Technol.*, **103**, 1 – 11 (2019) (<https://doi.org/10.1007/s00170-019-03329-6>).
10. F. Klocke, *Manufacturing Processes 1: Cutting*, Springer-Verlag, Berlin, Germany (2011) (ISBN 978-3-642-11978-1; DOI 10.1007/978-3-642-11979-8).
11. N. Zubkov, V. Poptsov, S. Vasiliev, and A. D. Batako, “Steel case hardening using deformational cutting,” *J. Manuf. Sci. Eng., Trans. Am. Soc. Mechan. Eng.*, **140**(6), Art. No. 061013 (2018) (DOI: 10.1115/1.4039382).
12. N. N. Zubkov, S. G. Vasil’ev, and V. V. Poptsov, “RF Patent 2556897 MPK C21D 8/00. Method of surface hardening strengthening with a cutting and deforming tool,” *Byull. Izobr. Polezn. Modeli*, No. 20 (2015), claim 01.21.2014, publ. 07.22.2015.
13. N. N. Zubkov, S. G. Vasil’ev, and V. V. Poptsov, “Features of quenching deformation cutting,” *Obrab. Met.*, **20**(2), 35 – 49 (2018) (DOI: 10.17212/1994-6309-2018-20.2-35-49).
14. A. G. Degtyareva, O. M. Zhigalina, D. N. Khmelenin, and V. N. Simonov, “Specifics of steel 35 structure after hardening by deforming cutting,” *Kristallografiya*, **64**(1), 120 – 126 (2019).